
Analysis Crystal Structure of $\text{La}_{0.7}(\text{Ba}_{1-x}\text{Sr}_x)_{0.3}\text{MnO}_3$ by Sol-Gel Method

Juli Hartati[†], Sitti Ahmiatri Saptari, Arif Tjahjono

Department of Physics, Faculty of Science and Technology, Syarif Hidayatullah Islamic State University,
Ir. H. Djuanda St, No.95, Cempaka Putih, Ciputat, South Tangerang, Banten 15412, Indonesia

[†]juli.hartati15@mhs.uinjkt.ac.id

Abstrak.

Penelitian tentang struktur kristal bahan $\text{La}_{0.7}(\text{Ba}_{1-x}\text{Sr}_x)\text{MnO}_3$ menggunakan metode *sol-gel* telah berhasil dilakukan. Bahan-bahan dasar yang digunakan dicampur di atas *hot plate* diaduk sambil ditetes *ammonia solution* sehingga mencapai pH 7, selanjutnya didiamkan sampai diperoleh bentuk gel. Gel dikeringkan pada suhu 120°C, selanjutnya dilakukan pra-kalsinasi dengan suhu 650°C selama 6 jam, dilanjutkan dengan kalsinasi pada suhu 1000°C selama 12 jam, dan kemudian disinter pada temperatur 1200°C selama 12 jam. Hasil *refinement* data XRD memberikan informasi bahwa struktur kristal $\text{La}_{0.7}(\text{Ba}_{1-x}\text{Sr}_x)\text{MnO}_3$ adalah rombohedral dengan *space grup* R-3c. Penambahan substitusi ion Sr^{2+} mengakibatkan terjadinya penurunan intensitas dan pergeseran puncak ke arah sudut yang lebih besar. Hal ini disebabkan karena pengaruh jari-jari ion Sr^{2+} yang lebih kecil dibandingkan dengan jari-jari ion Ba^{2+} .

Kata kunci: $\text{La}_{0.7}(\text{Ba}_{1-x}\text{Sr}_x)\text{MnO}_3$, metode sol-gel, struktur kristal

Abstract.

In this research, $\text{La}_{0.7}(\text{Ba}_{1-x}\text{Sr}_x)_{0.3}\text{MnO}_3$ compound ($x = 0; 0.2; 0.3; \text{ and } 0.5$) by sol-gel method has been investigated. The compound used is mixed on a hot plate until reached a pH 7 when dropped ammonia solution, then let stand until turn into a gel. Dehydrated gel at 120°C, pra-calcination at 650°C for 6 hours, calcination t 1000°C for 12 hours, and sintering at 1200°C for 12 hours. The result of refinement XRD pattern shown that samples are single phase with rhombohedral crystal structure with R-3c space group. The intensity decrease and peak list shift to larger angle when Sr-substitution increased, it's caused ionic radii of Sr^{2+} is smaller than Ba^{2+} .

Keywords: $\text{La}_{0.7}(\text{Ba}_{1-x}\text{Sr}_x)\text{MnO}_3$, sol-gel method, crystal structure

DOI : [10.15408/fiziyah.v1i1.15029](https://doi.org/10.15408/fiziyah.v1i1.15029)

INTRODUCTION

LaMnO_3 perovskite is one of the most interested engineering materials for researchers because unusual their electrical and magnetic properties. This structure can be modified through doping of divalent ion at La-site and transition ion at Mn-site. Substituted La-site with divalent ion such as Ba, Sr, and Ca can change Mn content from Mn^{3+} to Mn^{4+} , this phenomena can be explain with double exchange (DE) effect [1- 2], a system by which electron mobility between the nearest Mn ions, preferably, those with aligned spins is preferred [3].

In general, crystal structure of LaMnO_3 compound is cubic. Their crystal structure can be change or distortion caused of divalent ions substituted at La-site. Distortion on perovskite structure occurs of different ionic radii or size mismatch at La-site and Jahn-Teller effect. The average size of the A-site cation that modified the Mn-O-Mn bond angle and Mn-O distances can control this distortion [4]. Goldschmidt tolerance factor (t) of perovskite compounds ABO_3 is commonly used to determine the stability of the geometry and crystal structure distortions. The t is defined by ratios of constituent ionic radii of A, B, and O which expressed by [5]:

$$t = \frac{(r_A + r_O)}{(r_{Mn} + r_O)\sqrt{2}} \quad (1)$$

where r_A are the average ionic radii on site A, r_{Mn} and r_O are the average ionic radii of the manganese and oxygen ions. The ideal perovskite compounds take on a cubic structure with $t = 1$. When the ratio of the ionic radii deviates from the ideal value $t \neq 1$, a geometric strain and distortion of crystal occur [5].

In the previous work of Ref. [6], substitutes Ba^{2+} ions to the LaMnO_3 compound ($\text{La}_{0.7}\text{Ba}_{0.3}\text{MnO}_3$) has a rhombohedral structure with R-3c space group. The structure of $\text{La}_{1-x}\text{Sr}_x\text{MnO}_3$ switch from orthorhombic to rhombohedral when Sr^{2+} concentration is rising [7]. McBride et.all [1] suggested that $\text{La}_{0.6}\text{Ba}_{0.4}\text{MnO}_3$ and $\text{La}_{0.6}\text{Sr}_{0.4}\text{MnO}_3$ have a synthesized LaMnO_3 rhombohedral structure using the same process. There are several methods have been reported can be used to synthesis of LaMnO_3 with substitution divalent ions such as sol-gel method, solid state reaction, solution combustion method, molten salt reaction, and hydrothermal method. Among these methods, the sol-gel method makes it easier to obtain highly crystalline nanoparticles with the smaller size and stoichiometry desired [8-10].

Analysis crystal structure and crystallographic characterization generally used X-ray diffractometer (XRD), this is non-destructive analytical technique [11]. The properties of polycrystalline materials depend on several things, such as the crystalline size. Using Scherrer equation, we can calculated the crystalline size expressed by[12-13].

$$D = \frac{k\lambda}{B\cos\theta} \quad (2)$$

where D is crystalline size, k have value 0.9, λ is wavelength of X-ray ($\lambda = 1.5406 \text{ \AA}$), B is FWHM, and θ is bragg angle.

In this work, $\text{La}_{0.7}(\text{Ba}_{1-x}\text{Sr}_x)_{0.3}\text{MnO}_3$ where ($x = 0; 0.2; 0.3$; and 0.5) have been synthesized by sol-gel method. Using Rietveld refinement of X-ray diffraction data the structural parameters (unit cell volume, crystalline size, bond length, bond angle, and tolerance factor (t)) were refined.

METHOD

$\text{La}_{0.7}(\text{Ba}_{1-x}\text{Sr}_x)\text{MnO}_3$ ($x = 0; 0.2; 0.3$; and 0.5) was prepared using the sol-gel reaction method, La_2O_3 (99.99%), $\text{Mn}(\text{NO}_3)_2 \cdot 4\text{H}_2\text{O}$ (98.5%), $\text{Ba}(\text{NO}_3)_2$ (99%), $\text{Sr}(\text{NO}_3)_2$ (99%), and $\text{C}_6\text{H}_8\text{O}_7 \cdot \text{H}_2\text{O}$ (99.5%). The compounds were mixed and stirred on the hot plate, then added ammonia solution during the stirring process and resulted in brown colloid, after that oven at 120°C for 3 hours. After drying, pra-calcined at 650°C for 6 hours and then calcined at 1000°C

for 12 h. The black powder obtained was pressed at 10 tons and sintered at 1200°C for 12 h. XRD Panalytical X'pert Pro MPD identified the crystal structure and phase information of the samples with Fast Detector X'celerator using CuK α ($\lambda = 1.5406 \text{ \AA}$) radiation in the range 10°-90° with step size of 0.02°. The X-ray diffraction data were analyzed by Rietveld refinement using HighScore Plus software.

RESULT AND DISCUSSION

XRD character trends in Fig. 1 shown the single phase of LBSMO where all samples have rhombohedral structure with R-3c space group. XRD results also indicated that the intensity decreased when Sr²⁺ substitution increased. The sample's unit cell parameters, other fitting parameter and Goldscmidt tolerance factor are shown in Table 1 using the refined crystallography data. Fig. 2 shown the peak LBSMO shifted to the right when substitution Sr²⁺ increased. The higher value of 2-theta indicates that LBMO ($x = 0$) have larger d-spacing compared to substituted with Sr²⁺ so d-spacing decreased, which is caused by the ionic radii of Sr²⁺ (1.44 Å) is smaller to replaces of Ba²⁺ (1.61 Å).

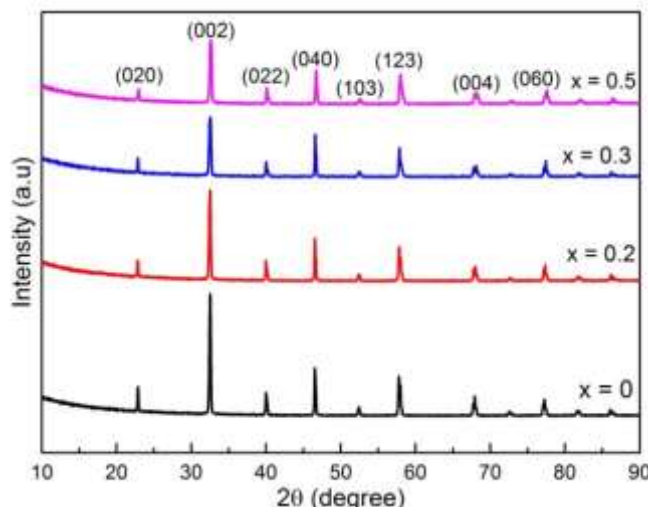


Figure 1. LBSMO XRD pattern

Table 1. Structure parameter La_{0.7}(Ba_{1-x}Sr_x)_{0.3}MnO₃

Lattice Parameters	$x = 0$	$x = 0.2$	$x = 0.3$	$x = 0.5$
a = b (Å)	5.538	5.544	5.540	5.543
C (Å)	13.501	13.465	13.475	13.425
<i>Discrepancy Factors</i>				
R _p	6.0042	6.0145	6.1213	6.336
W _r _p	7.852	8.067	8.121	8.392
GOF	1.18	1.204	1.31	1.35
<i>Goldscmidt tolerance factor</i>				
<i>t</i>	0.9885	0.9848	0.9832	0.9794

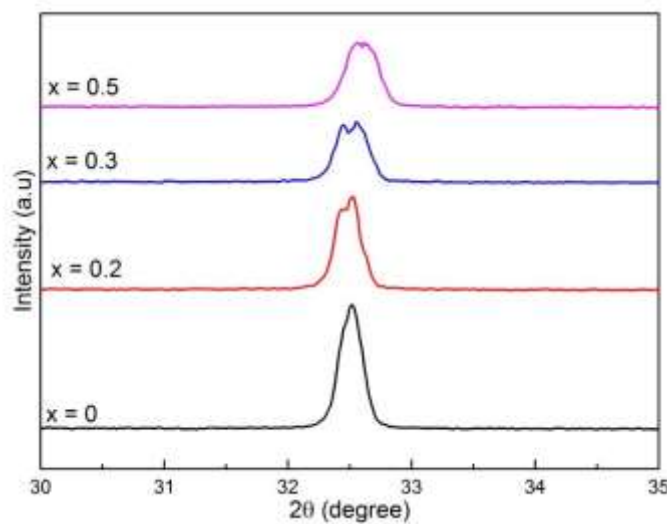


Figure 2. Shifting of peak LBSMO

Beside the result of refinement in table 1, substituted Sr^{2+} also caused a decrease of volume cell crystal shown fig. 3, it's occurred that ionic radii of Sr^{2+} smaller than ionic radii of Ba^{2+} so the d-spacing is decreased. The different ionic radii also affected Goldschmidt tolerance factor (t) as a result distortion of LaMnO_3 structure caused mismatch between ionic radii which is substituted with the ionic radii of La. The ionic radii of Ba^{2+} (1.61 Å) and Sr^{2+} (1.44 Å) too large to occupied site La (1.172 Å). Substitution increased causes the value of Goldschmidt tolerance factor decreased. This occurred when substituted increased, the value of ionic radii at site A from $\text{La}_{0.7}(\text{Ba}_{1-x}\text{Sr}_x)_{0.3}\text{MnO}_3$ decreased from 1.435 Å to 1.4025 Å. Fig. 4 shown the crystalline size of $\text{La}_{0.7}(\text{Ba}_{1-x}\text{Sr}_x)_{0.3}\text{MnO}_3$ calculated using the Eq.(2).

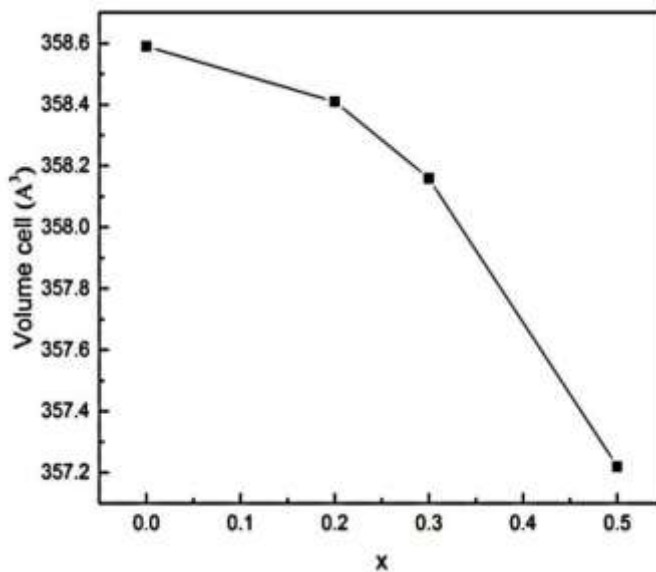


Figure 3. Volume cell of $\text{La}_{0.7}(\text{Ba}_{1-x}\text{Sr}_x)_{0.3}\text{MnO}_3$

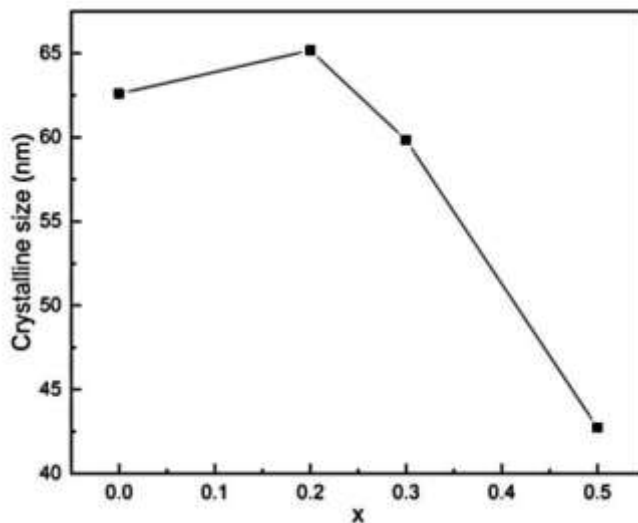


Figure 4. Crystalline size of $\text{La}_{0.7}(\text{Ba}_{1-x}\text{Sr}_x)_{0.3}\text{MnO}_3$

Sr^{2+} substituted on $\text{La}_{0.7}(\text{Ba}_{1-x}\text{Sr}_x)_{0.3}\text{MnO}_3$ not change crystal structure of LBSMO compound, but changed the lattice parameter and caused MnO_6 distortion. Bond length $d_{\text{Mn}-\text{O}}$ and bond angle $\langle \text{Mn}-\text{O}-\text{Mn} \rangle$ of $\text{La}_{0.7}(\text{Ba}_{1-x}\text{Sr}_x)_{0.3}\text{MnO}_3$ shown in fig 5. The increased substitution caused bond length increased and bond angle decreased.

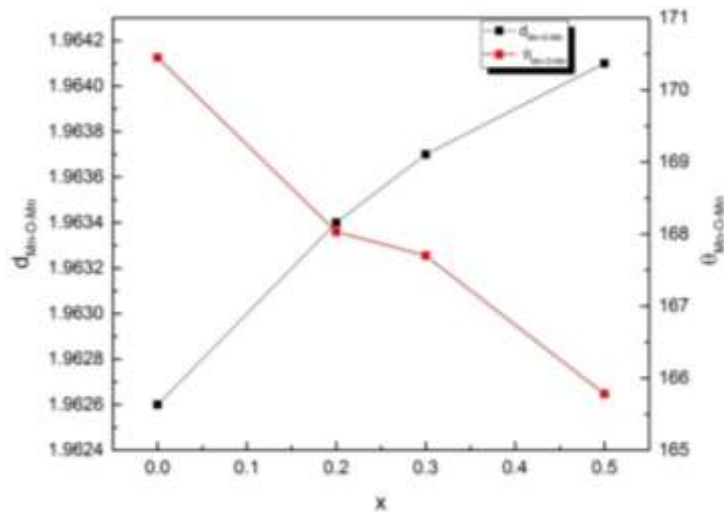


Figure 5. Bond length and bond angle

As the result refinement and Goldscmidt tolerance factor, crystal structure $\text{La}_{0.7}(\text{Ba}_{1-x}\text{Sr}_x)_{0.3}\text{MnO}_3$ is rhombohedral with R-3c space group. Using VESTA software, the visualization of $\text{La}_{0.7}(\text{Ba}_{1-x}\text{Sr}_x)_{0.3}\text{MnO}_3$ shown at fig. 6.

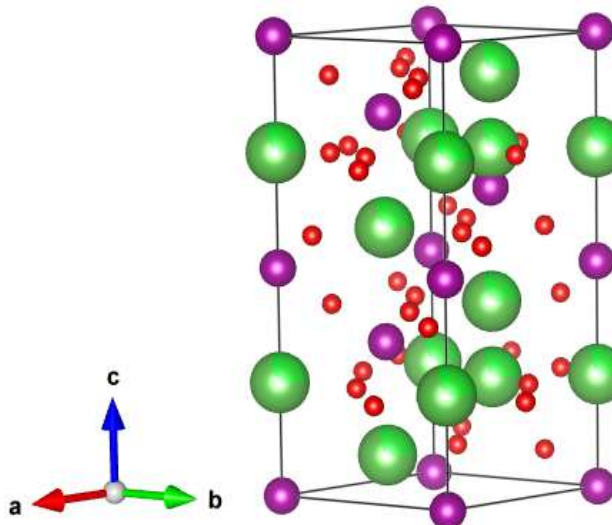


Figure 6. Visualization crystal structure of $\text{La}_{0.7}(\text{Ba}_{1-x}\text{Sr}_x)_{0.3}\text{MnO}_3$

CONCLUSION

Analysis of $\text{La}_{0.7}(\text{Ba}_{1-x}\text{Sr}_x)_{0.3}\text{MnO}_3$ crystal structure was studied using sol-gel method. All samples have rhombohedral structure with R-3c space group. Volume cell, crystalline size, and tolerance factor (t) are decreased with increasing Sr^{2+} substituted. On the other, the increased substitution of Sr^{2+} caused bond length $d_{\text{Mn-O}}$ increased and bond angle $\theta_{\text{Mn-OMn}}$ decreased.

REFERENCES

- [1] K. McBride, N. Partridge, S. Bennington-gray, S. Felton, L. Stella, and D. Pouliadi, "Synthesis, characterisation and study of magnetocaloric effects (enhanced and reduced) in manganate perovskites," *Mater. Res. Bull.*, vol. 88, pp. 69–77, 2017.
- [2] H. Rahmouni, A. Dhahri, and K. Khirouni, "The effect of tin addition on the electrical conductivity of Sn-doped LaBaMnO_3 ," *J. Alloys Compd.*, vol. 591, pp. 259–262, 2014.
- [3] J. F. Jurado and J. A. Játiva, "Metal-insulator transition and hopping conduction mechanisms in the $\text{La}_{0.7}\text{Ba}_{0.3}\text{MnO}_3$ compound," *J. Magn. Magn. Mater.*, vol. 335, pp. 6–10, 2013.
- [4] G. L. Reddy, Y. K. Lakshmi, N. Pavan, S. M. Rao, and P. V. Reddy, "Journal of magnetism and magnetic materials thermopower studies of rare earth doped lanthanum barium manganites," *J. Magn. Magn. Mater.*, vol. 362, pp. 20–26, 2014.
- [5] T. Sato, S. Takagi, S. Deledda, B. C. Hauback, and S. Orimo, "Extending the applicability of the goldschmidt tolerance factor to arbitrary ionic compounds," *Nat. Publ. Gr.*, no. March, pp. 1–10, 2016.
- [6] A. E. M. A. Mohamed, V. Vega, M. Ipatov, A. M. Ahmed, and B. Hernando, "Magnetoresistive and magnetocaloric response of manganite/insulator system," *J. Alloys Compd.*, vol. 657, pp. 495–505, 2016.
- [7] P. Yu, A. A. Naberezhnov, V. I. Nizhankovskii, and R. F. Mamin, "Temperature evolution of the magnetic properties of lanthanum-strontium manganites," *St. Petersbg. Polytech. Univ. J. Phys. Math.*, vol. 2, no. 3, pp. 175–180, 2016.
- [8] K. Navin and R. Kurchania, "The effect of particle size on structural, magnetic and transport properties of $\text{La}_{0.7}\text{Sr}_{0.3}\text{MnO}_3$ nanoparticles," *Ceram. Int.*, 2017.
- [9] H. Ahmad and R. Shreeja, "Comparative study on multifunctional behaviour of rare earth manganites with micro and nano grain size," pp. 3795–3800, 2014.
- [10] M. Kaenka *et al.*, "Magnetic properties of $\text{La}_{1-x}\text{Sr}_x\text{MnO}_3$ nanoparticles prepared in a molten salt," vol. 525, no. May, pp. 2012–2015, 2014.
- [11] M. Bortolotti, L. Lutterotti, and G. Peponi, "Combining XRD and XRF analysis in one rietveld-like fitting," no. April, 2017.

- [12] M. Aure and M. Sasaki, "The scherrer equation and the dynamical theory of x-ray diffraction," no. 1, pp. 1–6, 2016.
- [13] C. Paper, D. Kumar, N. Verma, C. B. Singh, and A. K. Singh, "Crystallite size strain analysis of nanocrystalline $\text{La}_{0.7}\text{Sr}_{0.3}\text{MnO}_3$ perovskite by williamson-hall plot method," no. December, pp. 3–8, 2017.